Fabrication of Modularly Functionalizable Microcapsules Using Protein-Based Technologies

HHS Public Access

Author manuscript

ACS Biomater Sci Eng. Author manuscript; available in PMC 2018 May 24.

Published in final edited form as:

ACS Biomater Sci Eng. 2016 November 14; 2(11): 1856–1861. doi:10.1021/acsbiomaterials.6b00447.

Fabrication of Modularly Functionalizable Microcapsules Using Protein-Based Technologies

Ashley C. Schloss[*],
Department of Molecular Biophysics and Biochemistry, Yale University, New Haven, CT 06511, USA

Wei Liu[*],
Department of Chemistry, Yale University, New Haven, CT 06511, USA

Danielle M. Williams[*],
Department of Molecular Biophysics and Biochemistry, Yale University, New Haven, CT 06511, USA

Gilad Kaufman,
Department of Chemical and Environmental Engineering, Yale University, New Haven, CT 06511, USA

Heidi P. Hendrickson,
Department of Chemistry, Yale University, New Haven, CT 06511, USA

Benjamin Rudshteyn,
Department of Chemistry, Yale University, New Haven, CT 06511, USA

Li Fu,
William R. Wiley Environment Molecular Sciences Laboratory and Physical and Computational Science Directorate, Pacific Northwest National Laboratory, P.O. Box 999, Richland, WA 99352, USA

Hongfei Wang,
Physical Sciences Division, Pacific Northwest National Laboratory, P.O. Box 999, Richland, WA 99352, USA

Victor S. Batista,
Department of Chemistry, Yale University, New Haven, CT 06511, USA

Chinedum Osuji,
Department of Chemical and Environmental Engineering, Yale University, New Haven, CT 06511, USA

Elsa C. Y. Yan, and
Department of Chemistry, Yale University, New Haven, CT 06511, USA

Correspondence to: Elsa C. Y. Yan; Lynne Regan.

[*]Contributed equally to this work

Author contributions:

All authors contributed to the design of the experiments. A.C.S., W.L., D.M.W., G.K., H.P.H, B.R., and L.F. executed the experiments. All authors assisted in writing the paper and data analysis.

Integrated Graduate Program in Physical and Engineering Biology, Yale University, New Haven, CT 06511, USA

Lynne Regan
Department of Molecular Biophysics and Biochemistry, Yale University, New Haven, CT 06511, USA

Department of Chemistry, Yale University, New Haven, CT 06511, USA

Integrated Graduate Program in Physical and Engineering Biology, Yale University, New Haven, CT 06511, USA

The controlled assembly of materials into functional two and three-dimensional structures and arrays has potential applications in areas as diverse as bio-sensing[1], light harvesting, point of care diagnostics, regenerative medicine[2], food science[3], and drug delivery[4]. Natural proteins exhibit a wide array of structures and functions, which can be co-opted to fabricate user-specified functional materials. Here, we describe the use of a bacterial hydrophobin, in combination with a versatile protein-protein conjugation scheme, to manufacture robust and readily functionalizable microcapsules.

The bacterial hydrophobin, biofilm surface layer protein A (BslA), forms a stable, ordered monolayer at air-water or air-oil interfaces[5–7]. The amphiphilic nature of BslA, which underlies such behavior, is evident from its 'bipartite' structure[7] - a hydrophilic, classical iG fold and a hydrophobic cap. (3 1a). Its potential as a surface coating and emulsifier is well documented[8].

Here, we describe a general strategy to incorporate function into BslA monolayers. We took advantage of the SpyCatcher–SpyTag system[9,10], which enables a spontaneous covalent isopeptide bond to be formed between a lysine side chain on the SpyCatcher protein and an aspartic acid side chain on the SpyTag peptide (Figure 1b). We genetically engineered constructs that fuse the 13-residue SpyTag peptide to either the N- or C- terminus of BslA (Figure 1c), separated by a flexible linker (GGSGGS). BslA modified with the SpyTag peptide may then be functionalized by reaction with any protein of interest expressed as a fusion protein with SpyCatcher.

BslA with SpyTag attached at either end is able to form monolayers at an air-water interface. Wild-type (WT) BslA forms a well-defined monolayer at an air-water interface, whose properties can be readily characterized using a Langmuir-Blodgett apparatus. We compared the behavior of BslA fused to SpyTag at either the N- or C-terminus with that of WT BslA, measuring surface pressure-area compression isotherms for each (Figure 2a). Monolayers formed by WT BslA or N- or C-terminally SpyTagged BslA all have collapsing surface pressures of ~65 mN/m, comparable to that of a typical phospholipid monolayer (55–65 mN/m). The limiting area of each monolayer was determined by extrapolation of the isotherm in the solid phase to zero surface pressure, giving values of 720 ± 12, 790 ± 4, and 900 ± 23 $Å^2$ for WT BslA, C-terminally SpyTagged BslA, and N-terminally SpyTagged BslA, respectively. Thus C-terminally SpyTagged BslA occupies a comparable surface area per molecule to that of WT BslA, whereas N-terminally SpyTagged BslA occupies a larger

area, suggesting that the N-terminal tag causes a greater perturbation to the uniform monolayer structure than does the C-terminal tag. Moreover, the slopes of the compression isotherms of both SpyTagged BslA proteins are smaller than that of WT BslA, suggesting that the SpyTagged BslA films are more compressible than the WT BslA film (Figure 2a). We investigated the possible structural changes that underlie these changes in the macroscopic physical properties by molecular dynamics simulations (*vide infra*).

Characterization of the self-assembled monolayers using nonlinear surface-specific vibrational sum frequency generation (SFG) spectroscopy[11–14] reveals the structural similarities and differences between the different BslA constructs. Using SFG to characterize protein structure in the monolayers, we observed that spectra in the amide I region for WT BslA, C-terminally SpyTagged BslA, and N-terminally SpyTagged BslA at an air-water interface show two peaks at ~1675 and ~1690 cm^{-1}, assigned to β-turns and to the B1 mode of antiparallel β-sheets, respectively (Figure 2b)[5], The peak at ~1690 cm^{-1}, which is characteristically narrow in WT BslA[5], is also narrow with a full-width-at-half-maximum of less than 10cm^{-1} (Supplementary Table 1) in the spectra of both C- and N-terminally SpyTagged BslA, indicating highly ordered structure; therefore this observation suggests that the presence of SpyTag at either end of BslA does not significantly perturb the ordered self-assembled structure at the interface. The SFG spectra in the C-H stretch region (Figure 2c) provide an indication of differences between the three proteins. Notably, the vibrational band of the symmetric methyl stretch for N-terminally SpyTagged BslA (~2884 cm^{-1}) was blue-shifted by ~10 cm^{-1} compared to that band in both WT BslA (~2876 cm^{-1}) and C-terminally SpyTagged BslA (~2875 cm^{-1}), see Supplementary Table 1.

To elucidate the potential origins of these differences we performed molecular dynamic (MD) simulations of WT BslA, N-terminally SpyTagged BslA, and C-terminally SpyTagged BslA. With N-terminally SpyTagged BslA, we observe that hydrophobic contacts are established between the side chains of SpyTag residues and side chains of the hydrophobic region of BslA (Supplementary Figure 1). By contrast, for C-terminally SpyTagged BslA we observe minimal interactions between residues in the SpyTag and BslA. The overall average fluctuations of BslA residues are increased as a result of adding the SpyTag at either the N- or C-terminus (Supplementary Table 2). However, when we examine the fluctuations in more detail, we find that fluctuations increase most in the hydrophobic region when BslA is SpyTagged at the N-terminus. Notably, methyl groups in the hydrophobic region are oriented along the principal axis of the protein (which we expect to be closely aligned to the surface normal) (Supplementary Figure 2), and methyl groups with this orientation contribute most strongly to the SFG signal under ssp polarization for the symmetric stretch. Thus, direct interactions between the N-terminal SpyTag and the methyl groups in the hydrophobic region of BslA (Figure 1c), evident in the MD simulations, may underlie the observed SFG spectral shifts.

The thin, uniform monolayer of BslA protein that is formed at an air-water or oil-water interface suggests that SpyTag peptides displayed by fusion to BslA will be readily accessible (Figure 1c). Having established that C-terminally SpyTagged BslA forms robust monolayers, we proceeded to use this protein to fabricate microcapsules. Using a microfluidic device (Figure 3a) (described in detail in Materials and Methods), we formed

oil-in-water microcapsules shown schematically in Figure 3b. Both WT BslA and a 3:1 mixture of WT BslA and C-terminally SpyTagged BslA form monodisperse microcapsules (Figure 3c) with mean diameters of 108 ± 2.4μm and 106 ± 3.7μm, respectively. Capsules formed from either WT BslA or a 3:1 mixture of WT BslA and C-terminally SpyTagged BslA (hereafter referred to as WT BslA capsules and SpyTagged BslA capsules, respectively) remain monodisperse and stable at room temperature for weeks.

SpyTagged BslA capsules can form a covalent linkage with a SpyCatcher-green fluorescent protein (GFP) fusion protein (Figure 4a and b). To enable us to readily visualize the product, we reacted C-terminally Spy-Tagged BslA with SpyCatcher-GFP fusion protein. Figure 4b shows the results of incubating WT BslA capsules and N-terminally SpyTagged BslA capsules with SpyCatcher-GFP. Only the capsules SpyTagged BslA capsules react to form a linkage with SpyCatcher-GFP that is resistant to washing. The attraction of labeling in this fashion is that the C-terminal Spytag does not perturb BslA's ability to self-associate at interfaces and to form robust capsules. Such capsules may then be covalently labeled with SpyCatcher fused to any protein of interest. For demonstration purposes we used SpyCatcher-GFP.

To directly confirm that C-terminally SpyTagged BslA forms a covalent bond with SpyCatcher, we fused Glutathione S transferase (GST) to C-terminally SpyTagged BslA (GST-BslA-SpyTag) and incubated it with SpyCatcher-GFP. The GST was fused to BslA to make the protein large enough to visualize on an SDS PAGE gel and also to prevent it from aggregating into inaccessible micelles. We analyzed the products of this reaction by boiling in SDS followed by SDS denaturing gel electrophoresis. The appearance of a new product, with a mobility consistent with a covalently linked GST-BslA-SpyTag and SpyCatcher-GFP, is clearly evident. GST-BslA alone does not form such a complex with SpyCatcher-GFP (Supplementary Figure 3).

In summary, we have demonstrated a simple strategy to prepare monolayers and microcapsules using C-terminally SpyTagged BslA. BslA modified in this fashion retains the structural and mechanical properties of WT BslA. Moreover, it can be functionalized by the covalent attachment of any desired protein fused to SpyCatcher. We demonstrate the methodology by functionalizing the SpyTagged BslA capsules with SpyCatcher-GFP, for ease of visualization. It is clear that this approach can be easily modified to attach a wide range of different proteins or peptides to the microspheres, such as ligands to important cellular biomarkers or receptors. One application we envision is the display of the extracellular domains of membrane proteins. This new class of functionalized surface arrays creates a novel platform for surface patterning, targeted drug delivery, and targeted imaging.

Methods

Cloning

The gene encoding $BslA_{29–176}$ was purchased from GenScript and cloned into the pGEX-6P-1 vector using the BamHI and XhoI restriction sites, to give a GST-fusion protein. There is a PreScission protease cleavage site between GST and BslA, which allows for removal of the GST tag during protein purification. The sequence encoding the SpyTag

peptide (AHIVMVDAYKPTK) was cloned onto either the 5’ or 3’ end of the BslA gene, to create a fusion protein that includes a 6 amino acid linker (GGSGGS) between the peptide and BslA. The gene for SpyCatcher was obtained from Addgene (pDEST14-SpyCatcher, Plasmid #35044). The SpyCatcher gene was added to the 3’ end of a gene encoding GFP and both genes were cloned into pPROEX HTa with a 6 amino acid linker (GGSGGS) between GFP and SpyCatcher. All cloning was performed using circular polymerase extension cloning (CPEC) unless otherwise stated[15].

Protein Expression and Purification

BslA proteins were expressed as fusion proteins with an N-terminal GST tag in BL21 (DE3) Gold cells. Five ml overnight cultures were added to 500 mL of Lysogeny-broth (LB) containing 100μg/mL ampicillin, grown at 37°C with shaking, and induced with 0.1mM isopropyl-β-thiogalactoside (IPTG) at OD_{600} of ~0.6–0.8. Cells were grown for a further 4 hours, then harvested by centrifugation. The cells were resuspended in 20mL lysis buffer (50 mM Tris, pH 7.4, 150 mM NaCl, 20 mg lysozyme) in the presence of EDTA-free Complete Protease Inhibitor (Roche), sonicated and cell debris was removed by centrifugation. Cell lysate was added to 3 mL of glutathione sepharose 4B resin (GE Healthcare Life Sciences) and allowed to bind for 1 hour at 4°C. The resin was washed with 10mL of lysis buffer, followed by 20mL wash buffer (50 mM Tris, pH 7.4, 150 mM NaCl, 1 mM EDTA, and 1 mM dithiothreitol), and eluted with 5 mL wash buffer plus 50 mM reduced glutathione. The eluted protein was dialyzed overnight at 4°C in the presence of PreScission protease (GE Healthcare Life Sciences) into storage buffer (10 mM phosphate buffer, pH 7.4, and 100 mM NaCl). The solution was incubated with 1 mL glutathione sepharose 4B resin and allowed to bind at 4°C for 1 hour to purify away cleaved GST and GST-tagged PreScission protease. Purified BslA was collected as the eluant.

SpyCatcher-GFP proteins were expressed as fusion proteins with an N-terminal hexahistidine tag in BL21 (DE3) Gold cells. Five mL overnight cultures were added to 500 mL of Lysogeny-broth (LB) containing 100μg/mL ampicillin, grown at 37°C with shaking, and induced with 1mM isopropyl-β-thiogalactoside (IPTG) at OD_{600} of ~0.6–0.8. Cells were shaken for a further 16 hours at 21°C, then harvested by centrifugation. Cells were then resuspended and incubated in lysis buffer on ice for 30 min in the presence of EDTA-free Complete Protease Inhibitor (Roche), and finally sonicated. Cell debris was removed by centrifugation and 5 mL of Nickel-NTA resin (Qiagen) equilibrated in buffer A (50 mM Tris, pH 7.4, 150 mM NaCl) containing 20 mM imidazole was added to the cell lysate and allowed to bind for 1 hour at 4°C. The resin was washed with approximately 20 mL of buffer A and then approximately 100 mL of buffer B (50mM Tris, pH 7.4, 300mM NaCl). The protein was eluted with buffer B containing 250 mM imidazole. Dialysis (into 50 mM Tris, pH 8.0, 150mM NaCl at 4°C) was used to remove imidazole.

Surface pressure-area isotherms

The surface pressure-area isotherms were obtained using a Langmuir trough (KN2002, KSV Instrument Ltd, Finland, illustrated in SI Scheme 1). Two symmetric Teflon barriers were controlled by the KSV Nima software. The surface pressure was measured using a Langmuir-Wilhelmy balance as a function of mean molecular area, which was calculated by

the software as the area between two barriers divided by the total numbers of molecules added to the system. The BslA solution was carefully spread onto the air-water interface and was allowed to equilibrate for 10 min, followed by compression using the barrier at a constant speed of 20 mm/min. For the surface pressure-area isotherms, the surface pressure was recorded as a function of mean molecular area until the collapse point is reached.

SFG spectrometer and spectral analyses

The SFG spectrometer used in this study was described in detail previously.[16–17] Briefly, the instrument consists of two Ti:Sapphire lasers. One (Coherent, Palo Alto, CA) generated 40 fs wide pulses at 800 nm with a frequency of 1 kHz and was used as the seed beam. The seed beam was then amplified and used to pump an OPERA-Solo optical parametric amplifier (OPA) to yield IR pulses at ~30 μJ/pulse at the C-H stretch region (2800–3000 cm^{-1}). The other laser (Coherent, Palo Alto, CA) generated visible 800 nm 100 ps wide pulses at 1 kHz and was amplified to yield a final energy of ~60 μJ/pulse. The two laser systems were electronically synchronized using Synchorlock-AP (Coherent, Palo Alto, CA) to an estimated jitter less than 200 fs. Both the IR and the visible beams overlapped temporally and spatially at the air-water interface to measure sample SFG response with the IR incident angle of 55° and the visible incident angle of 45° relative to the surface normal. Reflective SFG responses were spectrally dispersed using a monochrometer (Andor Technology, Belfast, NIR, Shamrock 750 mm, 1200 lines/mm grating) and measured using a CCD camera (Andor Technology, Newton 971P, back-illuminated). All reported SFG spectra were obtained using ssp polarization configuration, that is s-polarized SFG, s-polarized visible, and p-polarized infrared (Supplementary Figure 4). S-polarized means the lights were linearly polarized along the direction that is perpendicular to the plane of light propagation, while p-polarized means the lights were linearly polarized along the direction that is within the plane of light propagation.

The obtained SFG spectra were fitted using the equation 1.

$$\chi^{(2)} = \chi^{(2)}_{NR} + \sum_q \chi^{(2)}_q = \chi^{(2)}_{NR} + \sum_q \frac{A_q}{\omega_{IR} - \omega_q + i\Gamma_q}. \quad \text{(eq. 1)}$$

where $\chi^{(2)}$ is the experimentally measured second-order susceptibility of an interface consisting of a non-resonant term, $\chi^{(2)}_{NR}$, and a sum of vibrationally resonant terms, $\chi^{(2)}_q$; and A_q is the amplitude, Γ_q is the damping factor, ω_q is the resonant frequency of the q^{th} vibrational mode, and ω_{IR} is the frequency of the incident IR beam.

Microfluidic device fabrication

A patterned silicon master mold was fabricated using standard photolithography methods[16]. A polydimethylsiloxane (PDMS) pre-polymer and curing agent (Sylgard 184, Dow Corning) were mixed at a 10:1 ratio, by weight, and the mixture degassed to remove bubbles. Before the mixture was poured onto the master mold, the master mold was exposed to octadecyltrichlorosilane (Sigma-Aldrich) in a closed container for 4 hours to prevent sticking of the PDMS to the master and allow easier peeling of the PDMS from the master

after curing. Next the PDMS mixture was cured at 90°C for 2.5 hours. To form the microfluidic channels, the PDMS replica and a glass slide were exposed to oxygen plasma for 30 seconds and bonded together. The height of the microfluidic device is 90 μm and the width of injection lines for the outer and inner phases are 164 μm and 190 μm, respectively. The flow focusing junction is 51 μm wide.

Surface treatment

The microfluidic devices are rendered hydrophilic by thermal immobilization of polyvinyl alcohol (PVA) onto the PDMS surface. Briefly, the microfluidic device is filled with 1 percent by weight PVA solution in water (87–90% hydrolysed, molecular weight 30,000–70,000, Sigma-Aldrich) and incubated for 20 min at room temperature. Then, vacuum is applied to remove the PVA solution and the device is baked at 120°C for 2 hours to thermally immobilize the PVA onto the PDMS surface.

Molecular dynamics simulation

Molecular dynamics simulations were carried out using the AMBER-ffSB14 force field as implemented in the NAMD software package[18]. The starting structure of WT BslA was obtained from PDB entry 4BHU (chain C)[19] and the starting structure of SpyTag was obtained from PDB entry 4MLS (chain B)[20]. These structures were further modified in order to agree with the form of the protein used in the experiments by replacing MLY (59, 130, 158) with LYS and MSE (82, 99) with MET in BslA, and by adding the missing LYS13 to SpyTag, using the Maestro software package[21]. The N- and C-terminally SpyTagged BslA systems were generated by first attaching the SGGSGG linker to the C- or N-terminus of SpyTag, and then attaching the SpyTag+linker to the BslA protein using Maestro with zwitterionic N- and C-termini. These initial structures were optimized using the Protein Preparation Wizard in Maestro to obtain remove any initial clashes[22]. Hydrogens and approximately 8,300 and 11,500 TIP3P water molecules were added to the WT BslA and SpyTagged BslA, respectively, using the AmberTools15 software package[23]. This modeling strategy allows us to make the best estimate of the ‘pre-assembly’ structure. In the future, more complex modeling will be used to model the structure at the air-water interface.

Prior to production runs, the systems were equilibrated by first optimizing the positions of the hydrogen atoms and water molecules (while constraining the protein heavy atom positions), and then slowly heating the system to 298 K in the NVT ensemble using Langevin dynamics. Harmonic restraints were added to the protein heavy atoms during the initial heating steps, and these were gradually removed as the temperature was increased. The systems were then equilibrated in the NPT ensemble at 298 K and 1.0 atm using the Langevin piston. Long-range electrostatic interactions were taken into account using the Particle Mesh Ewald method, and van der Waals interactions were calculated using a switching distance of 10.0 Å and a cutoff of 12.0 Å. The integration time step was 1 fs. Production runs were 15 ns long, and the last 10 ns were used for analysis. Analysis of hydrophobic contacts and methyl orientations was carried out using the VMD software package in combination with in-house scripts[24].

The x-ray crystal structure of BslA has an asymmetric unit that contains 10 molecules of the protein. For the MD simulations, we used BslA chain C, which has the most complete structure. In the MD simulations of WT BslA, multiple configurations of the β-3 strand (within the hydrophobic region) are sampled, consistent with differences observed in the crystal.

Decoration of microcapsules with GFP

To decorate microcapsules, WT BslA and C-terminally SpyTagged BslA microcapsules were pipetted into separate solutions of 200μL of ~25 μM SpyCatcher-GFP protein and incubated for 10 min at room temperature. The SpyCatcher-GFP solution was removed by pipetting and the capsules were washed with 600 μL of deionized water. Microcapsules were imaged after incubation and each wash step using fluorescent confocal microscopy. The microscope is an inverted Nikon Eclipse Ti-S microscope and images were taken using a GFP filter cube set (49002-ET-EGFP (FITC/Cy2) (Chroma Technology Corp)), a Nikon E Plan 40X, 0.65 NA air objective, and an Andor Zyla 5.5 sCMOS camera.

Supplementary Material

Refer to Web version on PubMed Central for supplementary material.

Acknowledgments

We thank Susan Pratt for helpful instruction and discussions regarding the use of the microscope. We gratefully acknowledge the Support from the NSF through the Yale Materials Research Science and Engineering Center (grant No. MRSEC DMR-1119826) and from the Raymond and Beverly Sackler Institute for Biological, Physical and Engineering Sciences. C. O. also acknowledge NSF support under CBET-1066904 and the facilities of the Yale Institute for Nano and Quantum Engineering (YINQE); E.Y. also acknowledges support from the NSF (CHE 1213362); L.R. also acknowledges support from the NSF (DMR 1307712). A.C.S. is supported by a National Science Foundation Graduate Research Fellowship. Part of this work was conducted at the William R. Wiley Environmental Molecular Sciences Laboratory (EMSL), a national scientific user facility located at the Pacific Northwest National Laboratory and sponsored by the Department of Energy's Office of Biological and Environmental Research (BER). V.S.B. acknowledges supercomputer time from the National Energy Research Scientific Computing Center (NERSC) and support from the National Institute of Health (NIH) grant 1R01GM10621-01A1.

References

1. Wang Z, Li C, Xu J, Wang K, Lu X, Zhang H, Qu S, Zhen G, Ren F. Bioadhesive microporous architectures by self-assembling polydopamine microcapsules for biomedical applications. Chem. Mater. 2015; 27:848–856.
2. Hernández RM, Orive G, Murua A, Pedraz JL. Microcapsules and microcarriers for in situ cell delivery. Adv. Drug Deliv. Rev. 2010; 62:711–730. [PubMed: 20153388]
3. Anal AK, Singh H. Recent advances in microencapsulation of probiotics for industrial applications and targeted delivery. Trends Food Sci. Tech. 2007; 18:240–251.
4. Zakharchenko S, Ionov L. Anisotropic liquid microcapsules from biomimetic self-folding polymer films. ACS Appl. Mat. Inter. 2015; 7:12367–12372.
5. Wang Z, Morales-Acosta MD, Li S, Liu W, Kanai T, Liu Y, Chen YN, Walker FJ, Ahn CH, Leblanc RM, Yan EC. A narrow amide I vibrational band observed by sum frequency generation spectroscopy reveals highly ordered structures of a biofilm protein at the air/water interface. Chem. Commun. 2016; 52:2956–2959.

6. Bromley KM, Morris RJ, Hobley L, Brandani G, Gillespie RM, McCluskey M, Zachariae U, Marenduzzo D, Stanley-Wall NR, MacPhee CE. Interfacial self-assembly of a bacterial hydrophobic. P. Nat. Acad. Sci. 2015; 17:5419–5424.
7. Hobley L, Ostrowski A, Rao FV, Bromley KM, Porter M, Prescott AR, MacPhee CE, van Aalten DM, Stanley-Wall NR. BslA is a self-assembling bacterial hydrophobin that coats the Bacillus subtilis biofilm. P. Nat. Acad. Sci. 2013; 110:13600–13605.
8. Stanley-Wall NR, MacPhee CE. Connecting the dots between bacterial biofilms and ice cream. Phys. Biol. 2015; 12:063001. [PubMed: 26685107]
9. Zakeri B, Fierer JO, Celik E, Chittock EC, Schwarz-Linek U, Moy VT, Howarth M. Peptide tag forming a rapid covalent bond to a protein, through engineering a bacterial adhesin. P. Nat. Acad. Sci. 2012; 109:E690–E697.
10. Zhang WB, Sun F, Tirrell DA, Arnold FH. Controlling macromolecular topology with genetically encoded Spytag–Spycatcher chemistry. J. Am. Chem. Soc. 2013; 135:13988–13997. [PubMed: 23964715]
11. Yan ECY, Fu L, Wang Z, Liu W. Biological macromolecules at interfaces probed by chiral sum frequency generation vibrational spectroscopy. Chem. Rev. 2014; 114:8471–8498. [PubMed: 24785638]
12. Shen YR. Surface properties can be probed by second-harmonic and sum-frequency generation. Nature. 1989; 337:519–525.
13. Eisenthal KB. Liquid interfaces probed by second-harmonic and sum-frequency spectroscopy. Chem. Rev. 1996; 96:1343–1360. [PubMed: 11848793]
14. Richmond GL. Molecular bonding and interactions at aqueous surfaces as probed by vibrational sum frequency spectroscopy. Chem. Rev. 2002; 102:2693–2724. [PubMed: 12175265]
15. Quan J, Tian J. circular polymerase extension cloning of complex gene libraries and pathways. PLoS ONE. 2009; 4:e6441. [PubMed: 19649325]
16. Velarde L, Zhang XY, Lu Z, Joly AG, Wang ZM, Wang H-F. Communication: Spectroscopic phase and lineshapes in high-resolution broadband sum frequency vibrational spectroscopy: Resolving interfacial inhomogeneities of "identical" molecular groups. J. Chem. Phys. 2011; 135:241102. [PubMed: 22225136]
17. Velarde L, Wang H-F. Capturing inhomogeneous broadening of the -CN stretch vibration in a langmuir monolayer with high-resolution spectra and ultrafast vibrational dynamics in sum-frequency generation vibrational spectroscopy (SFG-VS). J. Chem. Phys. 2013; 139:084204. [PubMed: 24006990]
18. Philips JC, Braun R, Wang W, Gumbart J, Tajkhorshid E, Villa E, Chipot C, Skeel RD, Kale L, Shulten K. Scalable molecular dynamics with NAMD. J. Comput. Chem. 2005; 26:1781–1802. [PubMed: 16222654]
19. Lahiri SD, Mangani S, Durand-Reville T, Benvenuti M, De Luca F, Sanyal G, Docquier JD. Structural insight into potent broad-spectrum inhibition with reversible recyclization mechanism: avibactam in complex with CTX-M-15 and Pseudomonas aeruginosa AmpC β-lactamases. Antimicrob. Agents Ch. 2013; 57:2496–2505.
20. Li L, Fierer JO, Rapoport TA, Howarth M. Structural Analysis and Optimization of the Covalent Association between SpyCatcher and a Peptide Tag. J. Mol. Biol. 2014; 426:309–317. [PubMed: 24161952]
21. Schrödinger Release 2016-1: Maestro, version 10.5. Schrödinger, LLC; New York, NY: 2016.
22. Sastry GM, Adzhigirey M, Day T, Annabhimoju R, Sherman W. Protein and ligand preparation: Parameters, protocols, and influence on virtual screening enrichments. J. Comput. Aid. Mol. Des. 2013; 27:221–234.
23. Case, DA., Berryman, JT., Betz, RM., Cerutti, DS., Cheatham, TE., III, Darden, TA., Duke, RE., Giese, TJ., Gohlke, H., Goetz, AW., Homeyer, N., Izadi, S., Janowski, P., Kaus, J., Kovalenko, A., Lee, TS., LeGrand, S., Li, P., Luchko, T., Luo, R., Madej, B., Merz, KM., Monard, G., Needham, P., Nguyen, H., Nguyen, HT., Omelyan, I., Onufriev, A., Roe, DR., Roitberg, A., Salomon-Ferrer, R., Simmerling, CL., Smith, W., Swails, J., Walker, RC., Wang, J., Wolf, RM., Wu, X., York, DM., Kollman, PA. AMBER 2015. University of California; San Francisco: 2015.

24. Humphrey W, Dalke A, Schulten K. VMD - Visual molecular dynamics. J. Molec. Graphics. 1996; 14:33–38.

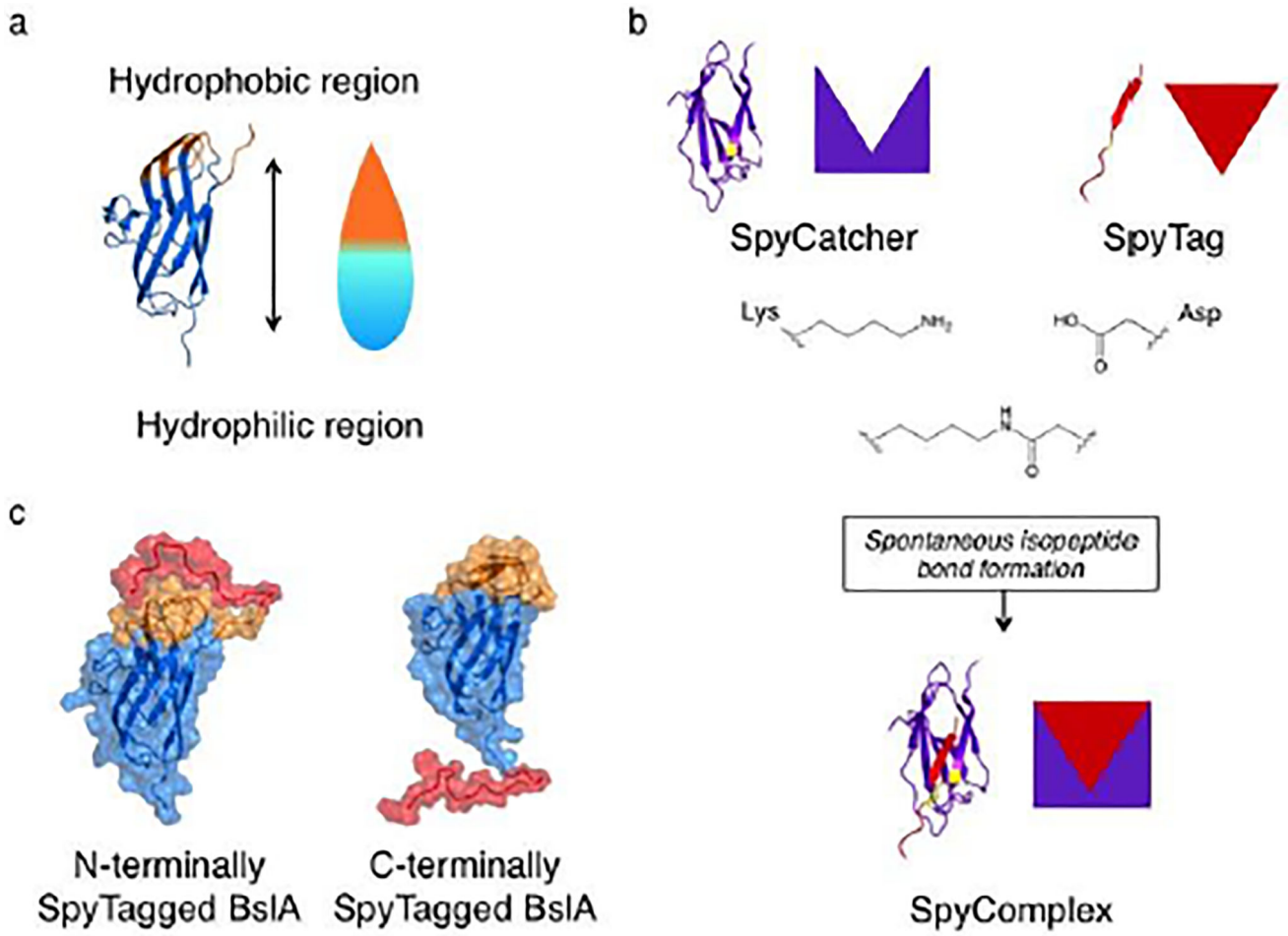

Figure 1.

Cartoon and ribbon representations of the protein building blocks. **a)** Ribbon representation and cartoon of the BslA protein. The orange coloring indicates the hydrophobic region, while the hydrophilic region is shown in blue. **b)** Ribbon and cartoon representation of SpyCatcher protein (purple) and SpyTag peptide (red). A lysine residue on the SpyCatcher protein and an aspartate residue on the SpyTag peptide spontaneously form a covalent isopeptide bond (residues contributing to the isopeptide bond colored in yellow), giving a covalently linked SpyTag-SpyCatcher complex. **c)** Representative snapshot from MD simulation for N-terminally SpyTagged BslA (left) and C-terminally SpyTagged BslA (right) with Connolly surfaces of the SpyTag (red) and the hydrophilic (blue) and hydrophobic (orange) regions of BslA.

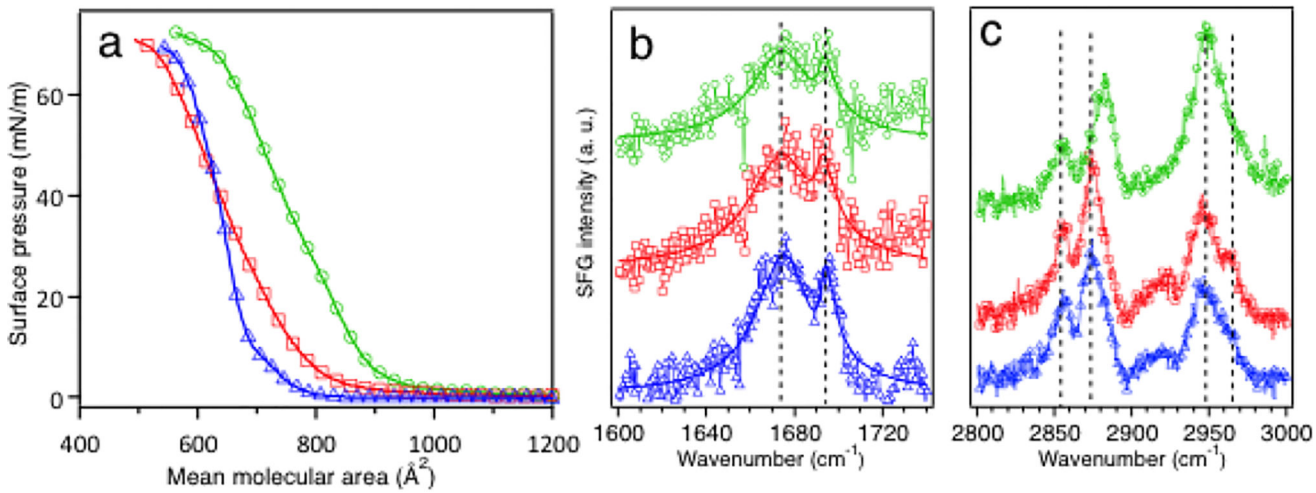

Figure 2.

Surface characterization of WT BslA (blue triangles), C-terminally SpyTagged BslA (red squares) and N-terminally SpyTagged BslA (green circles) at the air-water interface. **a)** Surface pressure-area isotherms measured using a Langmuir-Blodgett apparatus. **b)** SFG spectra of BslA proteins, showing the Amide I region. To aid comparison, dashed lines indicate 1675 and 1690 cm^{-1}. **c)** SFG spectra of BslA proteins showing the C-H stretch region. Dashed lines indicate 2875, 2884, and 2942 cm^{-1}. All SFG spectra were acquired using ssp polarization (s-polarized SFG, s-polarized visible, and p-polarized infrared). Results of spectral fitting are shown in Supplementary Table 1.

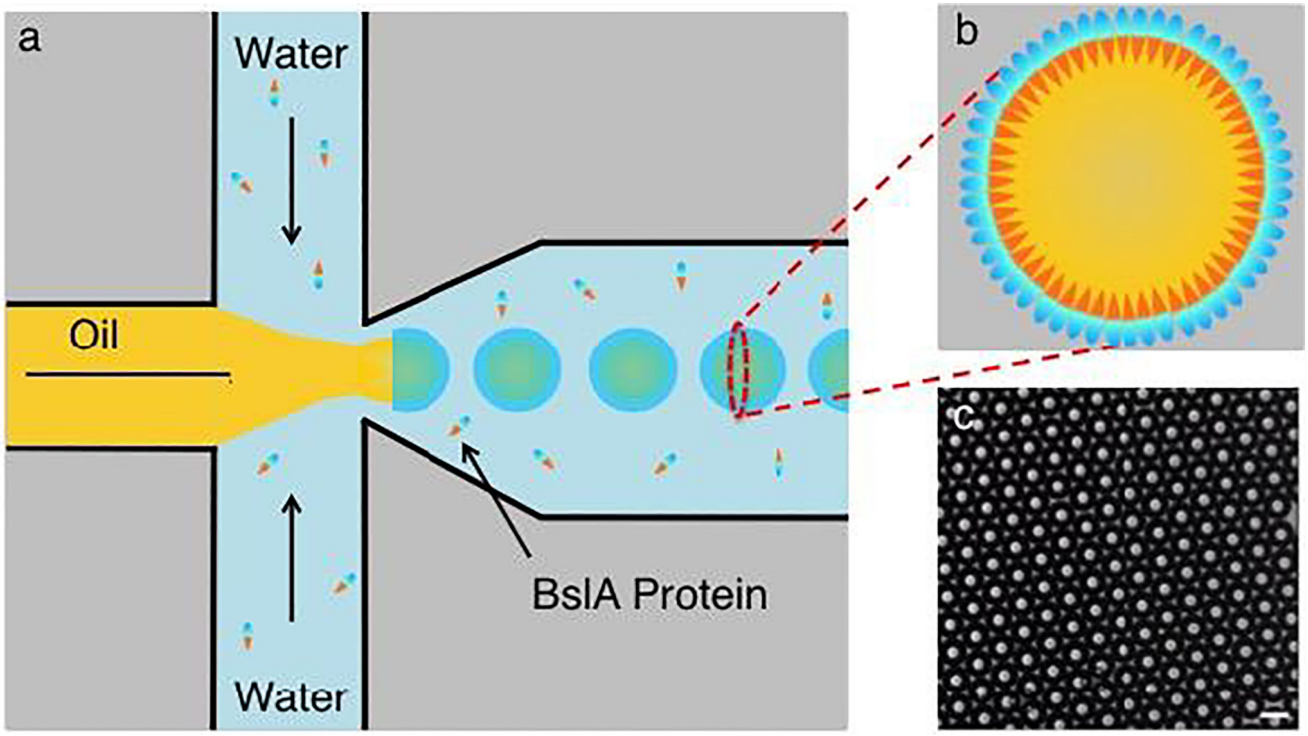

Figure 3.

Schematic illustration of the BslA capsule fabrication. **a)** Schematic illustration of the key region of the microfluidics device (not to scale, see materials and methods for details). Aqueous phase (light blue) containing BslA protein (blue-orange) and an oil phase (yellow) are brought into contact to form an oil-core microcapsule with a protein shell. **b)** Schematic illustration of a cross-section of an oil-filled BslA capsule. The hydrophobic end of BslA (orange) faces inwards, interacting with the oil and the hydrophilic end (blue) faces outwards, interacting with the aqueous phase. **c)** Brightfield images of stable oil-in-water capsules formed with WT BslA. Scale bar is 100 μm.

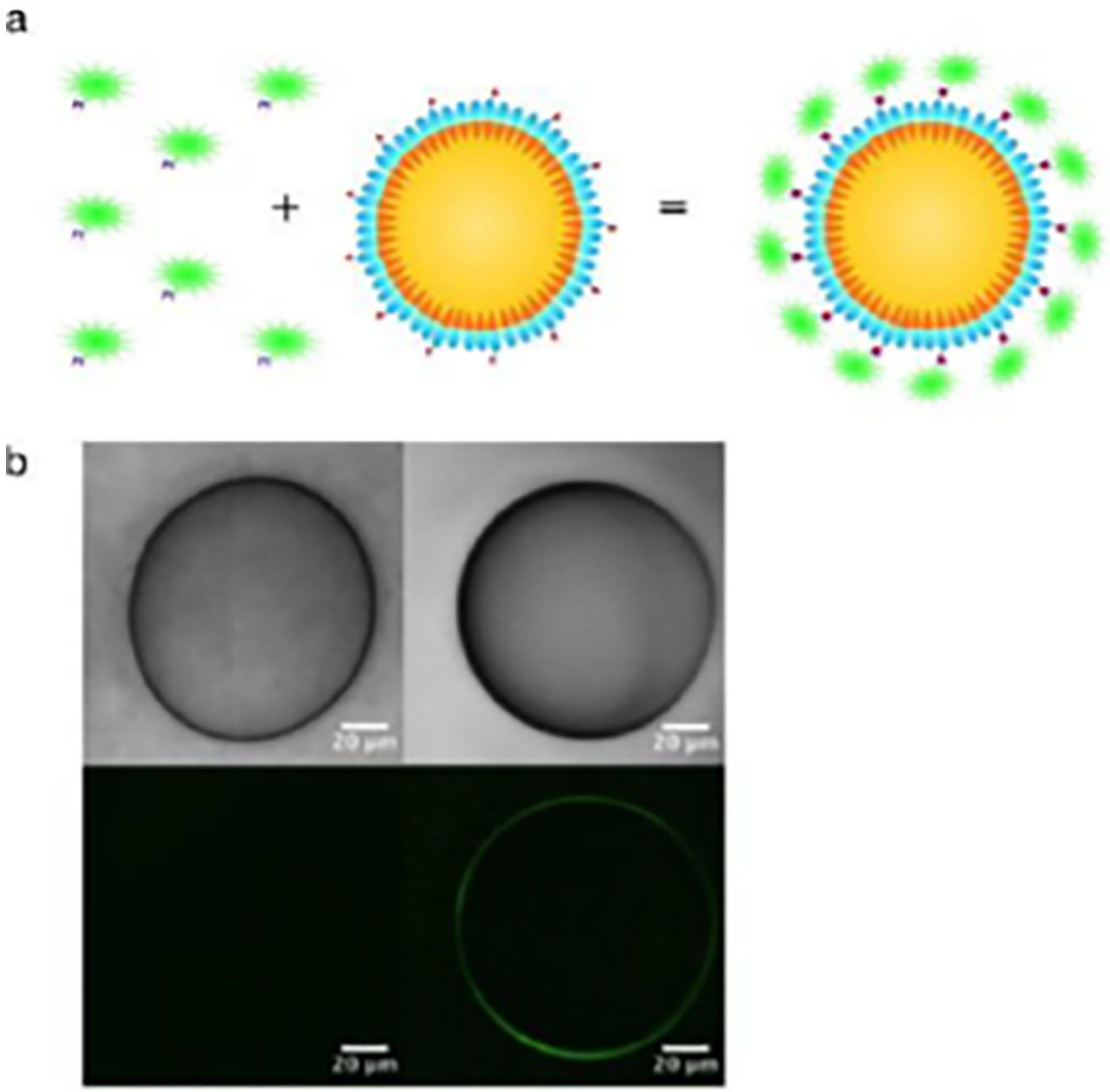

Figure 4.

a) Cartoon illustration of the decoration of microcapsules formed from C-terminally SpyTagged BslA by reaction with SpyCatcher-GFP. **b)** Brightfield and fluorescent images of wild type BslA and C-terminally SpyTagged BslA after reaction with SpyCatcher-GFP. **Top:** Confocal microscope brightfield images of WT BslA (left) and C-terminally SpyTagged BslA (right) microcapsules. **Bottom:** Fluorescent images of the capsules after a 10 min incubation with SpyCatcher-GFP followed by washing with water, of WT BslA (left) and C-terminally Spytagged BslA (right). GFP labeling of the capsules only occurs via the SpyTag-SpyCatcher reaction.